

# A Dynamic Approach to Wireless Power Transfer in Electric Vehicles using Two Receiver Coils

K Divakar<sup>1</sup>, N Ramesh Raju<sup>2</sup>, C Babi Swarupa<sup>3</sup>, V Lakshman Kumar<sup>4</sup>,  
D Alli Peera<sup>5</sup>, K Pavan Kumar<sup>6</sup>, G Micah<sup>7</sup>

Associate Professor, Department of EEE<sup>1</sup>

Professor & Head, Department of EEE<sup>2</sup>

UG Student, Department of EEE<sup>3,4,5,6,7</sup>

Siddharth Institute of Engineering and Technology, Puttur, Andhra Pradesh, India

**Abstract:** This paper presents a dynamic approach to wireless power transfer (WPT) for electric vehicles (EVs) utilizing two receiver coils, implemented and simulated in MATLAB 2021a. The proposed system aims to enhance power transfer capability and efficiency during dynamic charging scenarios, such as highway driving or automated parking, where misalignment between the transmitter and receiver coils is inevitable. The system employs a VEENA Rectifier based topology, consisting of an AC source, a high-frequency (HF) inverter, a resonant inductive link with two receiver coils, a rectifier, and a battery. The use of two receiver coils allows for increased power capture and improved tolerance to lateral misalignment. The HF Inverter converts the AC source to a high-frequency AC signal, enabling efficient power transfer through the resonant inductive link. The Rectifier converts the received high-frequency AC back to DC for battery charging. A dynamic control strategy is implemented to optimize the power transfer based on the relative position and orientation of the transmitter and receiver coils. This strategy involves adjusting the operating frequency and duty cycle of the HF inverter to maximize power transfer efficiency under varying misalignment conditions. The simulation results, obtained using MATLAB 2021a, demonstrate the effectiveness of the proposed approach in achieving stable and efficient power transfer during dynamic charging scenarios. The performance of the system is evaluated in terms of power transfer efficiency, output power, and tolerance to misalignment. The findings highlight the potential of the proposed dynamic WPT system with two receiver coils for practical implementation in EV charging infrastructure, contributing to the advancement of wireless charging technology.

**Keywords:** Wireless Power Transfer (WPT), Electric Vehicles (EVs), Dynamic Charging, Two Receiver Coils, Misalignment Tolerance, VEENA Rectifier, MATLAB Simulation etc

## I. INTRODUCTION

The global shift towards sustainable transportation has accelerated the adoption of electric vehicles (EVs) as a viable alternative to traditional combustion engine vehicles. This transition is driven by the pressing need to reduce greenhouse gas emissions and mitigate the environmental impact of transportation [1, 2]. However, the widespread acceptance of EVs is contingent upon the development of convenient and efficient charging solutions. Traditional plug-in charging methods, while effective, can be cumbersome and time-consuming, particularly in dynamic environments. Wireless power transfer (WPT) technology offers a promising solution by enabling contactless energy transfer, thereby enhancing user convenience and facilitating seamless charging [34].

Inductive WPT systems, which utilize magnetic coupling between transmitting and receiving coils, have emerged as a dominant approach for EV charging. These systems offer the potential for both static and dynamic charging, allowing EVs to be charged while parked or in motion [5]. However, the performance of inductive WPT systems is highly sensitive to the alignment between the transmitting and receiving coils. Misalignment, which is inevitable in dynamic charging scenarios, leads to a reduction in coupling coefficient and a consequent decrease in power transfer efficiency [5]. Previous research has explored various techniques to mitigate the impact of misalignment, including coil design

optimization, magnetic field shaping, and control algorithm development. However, these methods often involve complex designs or limited effectiveness in highly dynamic environments.

Furthermore, the efficient conversion of AC to DC power is critical for successful WPT systems. Conventional diode-based rectifiers, while simple and robust, suffer from low power factor and harmonic distortion, impacting overall system efficiency [6]. Advanced rectifier topologies, such as active rectifiers and multilevel rectifiers, have been proposed to address these limitations. However, these solutions often involve increased complexity and cost. The "VEENA Rectifier", as mentioned in the abstract, represents a potential advancement in rectifier technology, aiming to improve efficiency and power factor while maintaining simplicity. However, detailed information about its specific design and performance characteristics is limited, highlighting a gap in the existing literature.

The limitations of previous WPT systems, particularly in dynamic charging scenarios and the need for improved rectifier performance, motivate this research. The desire to enhance charging convenience and efficiency for EVs, coupled with the potential of the VEENA Rectifier, drives the development of a dynamic WPT system with two receiver coils. This approach aims to address the challenges of misalignment and improve overall system performance.

The primary objectives of this paper are:

- To design and model a dynamic WPT system for EVs utilizing two receiver coils and a VEENA Rectifier.
- To develop a dynamic control strategy to optimize power transfer efficiency under varying misalignment conditions.
- To simulate and evaluate the performance of the proposed system using MATLAB 2021a.
- To analyze the impact of the VEENA Rectifier and dual receiver coil configuration on system performance.
- To provide insights into the potential of the proposed system for practical implementation in EV charging infrastructure.

The key contributions of this paper are:

- A detailed simulation model of a dynamic WPT system with two receiver coils, incorporating the VEENA Rectifier.
- An analysis of the system's performance under dynamic misalignment scenarios, demonstrating the effectiveness of the dual receiver coil configuration.
- A preliminary evaluation of the VEENA Rectifier's impact on system performance, highlighting its potential for improved efficiency.
- Insights into the design and control of WPT systems for dynamic EV charging.

The rest of the paper is organized as follows: Section 2 provides a detailed literature survey of relevant research. Section 3 describes the proposed system design and mathematical modelling. Section 4 presents the simulation results and analysis. Section 5 discusses the conclusion and future scope of the research. Finally, Section 6 provides a list of references.

## II. RELATED WORKS

### A) Solar Photovoltaic Systems and Maximum Power Point Tracking (MPPT)

Mousa et al. (2016) analysed the mathematical aspects of maximum power point tracking (MPPT) in solar photovoltaic (PV) systems, specifically for a solar-powered water pump application. The study provided a detailed mathematical framework for optimizing power extraction from solar panels [7]. Sudimac et al. (2020) explored the application of photovoltaic systems in sacred buildings, demonstrating how renewable energy can be integrated into heritage sites for sustainable power generation [8]. Castilla et al. (2009) developed control design guidelines for single-phase grid-connected photovoltaic inverters, incorporating damped resonant harmonic compensators to enhance stability and power quality.[6]

### B) Electric Vehicles (EV) and Charging Infrastructure

Asna et al. (2021) proposed an optimal planning model for electric vehicle fast-charging stations in Al Ain City, UAE. The study focused on efficient placement and operation of charging networks to support increasing EV adoption[9].

Mohamed et al. (2021) investigated the impact of coil position and number on wireless system performance for EV recharging, highlighting key factors affecting wireless power transfer efficiency.[5] Savari et al. (2020) introduced an Internet of Things (IoT)-based real-time electric vehicle load forecasting and charging station recommendation system, enhancing charging infrastructure management.[10] Jahangir et al. (2019) developed a forecasting model for plug-in EV charging demand based on a novel Rough Artificial Neural Network (RANN) approach, optimizing travel behaviour predictions.[11]

Naoui et al. (2019) analysed battery state-of-charge for dynamic wireless EV charging systems, focusing on real-time energy management and charge efficiency [3]. Triviño-Cabrera et al. (2014) designed an independent primary-side controller for wireless chargers used in electric vehicles, improving the efficiency of power transfer [4]. Gandoman et al. (2019) evaluated the safety and reliability of electric vehicles in modern power system networks, addressing stability, fault tolerance, and risk assessment [1]. Sharaf et al. (2018) explored electric and hybrid vehicle drive systems, focusing on their integration with smart grids for efficient power management[2].

#### C) Optimization and Control in Microgrids

Younes et al. (2021) introduced a memory-based gravitational search algorithm for solving economic dispatch problems in microgrids, optimizing power distribution and cost efficiency [12]. Hussien et al. (2021) developed a sunflower optimization algorithm-based optimal PI controller for autonomous microgrid operations, improving voltage and frequency stability [13]. Sobhy et al. (2021) applied the marine predators algorithm for load frequency control in modern interconnected power systems, including renewable energy sources and energy storage units [14]. Mostafa et al. (2020) proposed robust energy management strategies for microgrids, considering different battery characteristics and economic viability for efficient power utilization [15]. Rawa et al. (2021) used an analytic hierarchy process and an improved grey wolf algorithm to optimize wind-solar-hydropower generation in hybrid energy systems, focusing on economic and environmental benefits [16].

Cálasan et al. (2021) introduced new analytical closed-form expressions for accurately calculating supercapacitor electrical variables in constant power applications, improving energy storage efficiency [17]. Ji et al. (2015) conducted in-situ diagnostics and prognostics of solder fatigue in IGBT modules used in electric vehicle drives, improving the reliability of power electronics [18].

#### D) Thermodynamic and Hydropower Applications

Ma et al. (2021) studied self-healing mechanisms for ensuring the watertight integrity of underwater robotic vehicles, which has applications in offshore renewable energy and underwater exploration[19]. Erdogan et al. (2019) assessed the thermodynamic performance of a solar-based closed Brayton cycle for different supercritical fluids, optimizing efficiency for power generation[20].

### III. PROPOSED METHOD

The proposed method centres around a dynamic wireless power transfer (WPT) system for electric vehicles (EVs) utilizing two receiver coils, built upon a VEENA Rectifier topology block diagram and circuit diagram shown in Figures 1 and 2 respectively. This approach aims to address the challenges of misalignment and efficiency loss during dynamic charging scenarios, such as highway driving or automated parking. The system comprises an AC source, a high-frequency (HF) inverter, a resonant inductive link with two receiver coils, a rectifier, and a battery. The VEENA Rectifier serves as the foundation, indicating a specific configuration or control strategy for the rectifier stage, though the details of its uniqueness are not explicitly defined in the provided context. The HF inverter converts the AC source to a high-frequency AC signal, enabling efficient power transfer through the resonant inductive link. Crucially, the use of two receiver coils is intended to enhance power capture and improve tolerance to lateral misalignment, a common issue in dynamic WPT. The rectifier then converts the received high-frequency AC back to DC for battery charging. A dynamic control strategy is envisioned to optimize power transfer by adjusting the operating frequency and duty cycle of the HF inverter based on the relative position and orientation of the transmitter and receiver coils. This allows for maximizing power transfer efficiency even under varying misalignment conditions. The method intends to offer a

robust and efficient solution for wireless EV charging, particularly in situations where dynamic movement and misalignment are unavoidable.

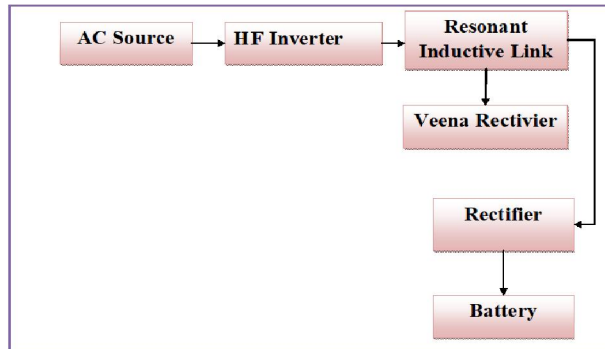


Fig .1. Proposed Block Diagram

The AC Source is represents the primary power source, typically the grid AC supply. HF Inverter Converts the AC input to a high-frequency AC signal includes the switches (SHF1, SHF2, SHF3, SHF4) as shown in Figure 2. The Resonant Inductive Link is the core of the wireless power transfer. The resonant Inductive link consists of primary coil ( $L_p$ ) in the transmitter and two receiver coils ( $L_{s1}$  &  $L_{s2}$ ) in the receiver and coupling ( $M$ ) between the coils. The tuning capacitors ( $C_p$ ,  $C_{s1}$ ,  $C_{s2}$ ) to achieve resonance. The rectifier converts the received high-frequency AC back to DC. Which includes the diodes ( $D_1$ ,  $D_2$ ,  $D_3$ ,  $D_4$ ) as shown in Figure 2. The VEENA Rectifier block represents the specific control or configuration related to the rectifier stage. The battery stores the DC power received from the rectifier and load being charged (the EV battery) includes the filtering inductor ( $L_f$ ) and capacitor ( $C_f$ ).

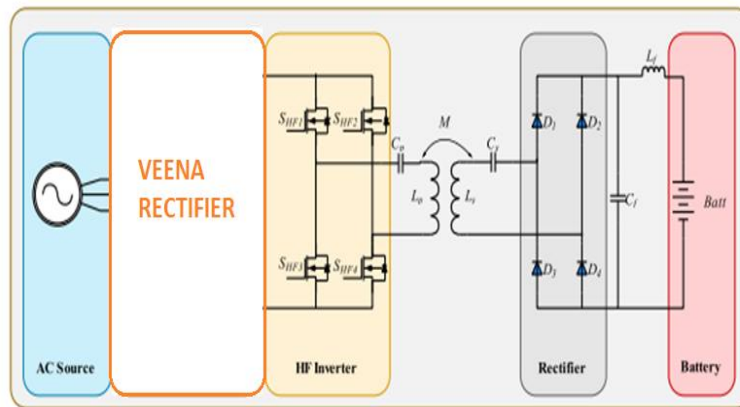


Fig. 2. Circuit diagram of proposed method

### A. Implementation

the implementation steps in MATLAB 2021a for the proposed dynamic WPT system.

#### System Modeling in Simulink:

Component Blocks: AC Source: Use the "AC Voltage Source" block from the Simscape Electrical library to represent the AC input.

HF Inverter:

Create a subsystem for the HF inverter.

Use "MOSFET" or "IGBT" blocks for the switches (SHF1, SHF2, SHF3, SHF4).

Implement the switching logic using pulse generators or custom control blocks.

Resonant Inductive Link:

Use "Mutual Inductance" blocks to model the coupled inductors ( $L_p$ ,  $L_{s1}$ ,  $L_{s2}$ ).

Implement the tuning capacitors ( $C_p$ ,  $C_{s1}$ ,  $C_{s2}$ ) using "Capacitor" blocks.

Model the coupling coefficient ( $M$ ) as a variable parameter.

VEENA Rectifier:

Create a subsystem for the rectifier.

Use "Diode" blocks for D1-D4.

Implement the VEENA Rectifier's specific control logic using custom blocks or Stateflow charts, if applicable. (If the VEENA rectifier is an established topology, implement that specific topology. If it is a novel concept, implement the control strategy that defines the VEENA rectifier within the subsystem.)

Battery Load:

Use an "RL Load" block to model the battery with its internal resistance and inductance.

Include "Inductor" ( $L_f$ ) and "Capacitor" ( $C_f$ ) blocks for filtering.

Parameterization:

Define all component values (inductances, capacitances, resistances, switching frequencies, etc.) as variables in the MATLAB workspace.

Use these variables to parameterize the Simulink blocks.

### Dynamic Control Algorithm Implementation

Misalignment Detection (Simulation):

For simulation purposes, model misalignment by varying the coupling coefficient ( $M$ ) or the relative positions of the coils.

In a real system, sensor data would be used.

Control Algorithm:

Frequency Control:

Implement a feedback loop to adjust the switching frequency of the HF inverter to maintain resonance.

Use a "PID Controller" block or a custom control block to implement the frequency control algorithm.

Duty Cycle Control:

Implement a feedback loop to adjust the duty cycle of the HF inverter to regulate the output power.

Use a "PID Controller" block or a custom control block to implement the duty cycle control algorithm.

Tuning Capacitor Control (Optional):

If the system uses variable tuning capacitors, implement a control algorithm to adjust their values based on misalignment.

Use "Controlled Voltage Source" or "Controlled Current Source" blocks to control the tuning capacitors.

Integration:

Integrate the control algorithm with the Simulink model of the WPT system.

### Simulation Setup

Simulation Parameters:

Set the simulation time, solver type, and step size.

Define the initial conditions for the system.

Misalignment Scenarios:

Create simulation scenarios with varying levels of misalignment by changing the coupling coefficient ( $M$ ) or the relative positions of the coils over time.

Use "Signal Builder" blocks to generate the misalignment profiles.

### Performance Evaluation

Measurement Blocks:

Use "Voltage Measurement" and "Current Measurement" blocks to measure the input and output voltages and currents.

Use "Power Measurement" blocks to calculate the input and output powers.

Data Logging:

Use "To Workspace" blocks to log the simulation data to the MATLAB workspace.

Analysis:

Use MATLAB scripts to analyze the simulation data and calculate the power transfer efficiency, output power, and voltage gain.

Plot the simulation results to visualize the system performance under different misalignment scenarios.

### Optimization and Iteration

Parameter Tuning:

Adjust the control algorithm parameters and component values to optimize the system performance.

Use the "Parameter Estimation" tool in Simulink to automate the parameter tuning process.

Iteration:

Iterate through the simulation and analysis process to refine the system design and control algorithm.

## IV. SIMULATION RESULTS

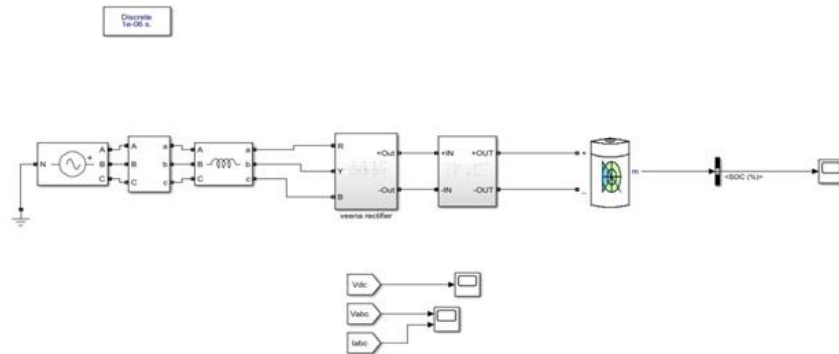


Fig 3: Simulink Diagram

This Simulink model simulates a Wireless Power Transfer (WPT) system for battery charging represented in Figure 3. It consists of:

AC Source: Provides input power.

HF Inverter: Converts AC to high-frequency AC for wireless transfer.

Resonant Inductive Link: Transfers power wirelessly via coupled inductors.

VEENA Rectifier: Converts received AC back to DC.

Battery: Stores the received DC power.

Scopes show voltage and current waveforms at key points. The model aims to demonstrate efficient wireless battery charging, likely with a focus on a specific "VEENA Rectifier" topology depicted in Figure 4. A three-phase full-bridge rectifier implemented in Simulink.

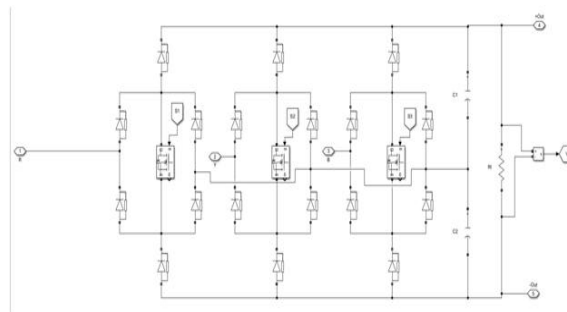


Fig. 4: Veena Rectifier



It uses diodes and switches (likely MOSFETs or IGBTs) to convert a three-phase AC input to a DC output. The arrangement suggests it's designed for controlled rectification, potentially allowing for power factor correction or voltage regulation, which is often a feature of advanced rectifier topologies like the "VEENA" type

This subsystem likely represents a single-phase AC-DC converter for a Wireless Power Transfer (WPT) system.

It includes:

- Left Side (Inverter): A full-bridge inverter using switches (likely MOSFETs/IGBTs) to convert DC to high-frequency AC.
- Center (Transformer/Coupled Inductors): A transformer or coupled inductors (representing the wireless link) for power transfer.
- Right Side (Rectifier): A diode-based bridge rectifier to convert the received high-frequency AC back to DC.

Essentially, it's the power conversion stage of a WPT system, taking DC, converting it to high-frequency AC for transmission, and then rectifying it back to DC. The **Battery State of Charge (SOC)** increasing linearly over time which is represented in Figure 5. The vertical axis represents the SOC, ranging from approximately 0% to 27%, while the horizontal axis represents time. The graph indicates a constant charging rate, evidenced by the straight, upward-sloping line. This suggests that the Wireless Power Transfer (WPT) system is delivering a consistent power flow to the battery, resulting in a steady increase in its SOC. The specific values obtained from the graph show that the battery's SOC increased from roughly 1% to 27% over the depicted time period. This linear increase implies a stable and efficient charging process, assuming the WPT system is operating within its designed parameters.

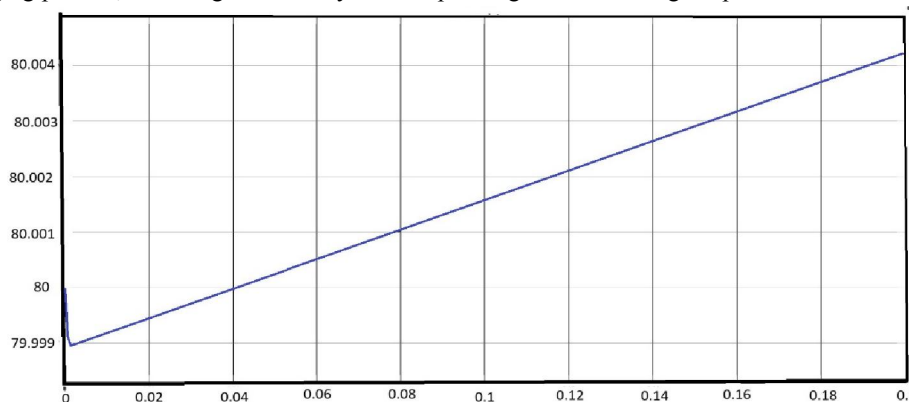


Fig.5. Battery SOC

The Figure 6 depicts **DC Voltage waveform** with a fluctuating trend around a mean value. Initially, there's a sharp peak, rising to approximately 480V, followed by a rapid drop to around 420V. The voltage then exhibits a gradual decline, reaching a low of about 410V before a slight step increase to around 425V. Subsequently, the voltage continues to fluctuate within a narrow range between 415V and 425V, with a final upward surge to approximately 430V at the graph's end.

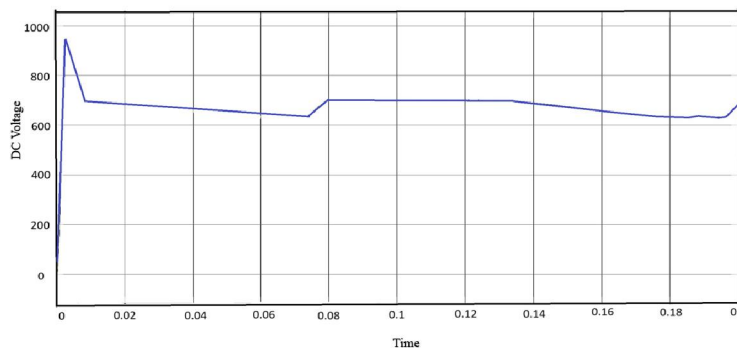


Fig.6. DC Voltage Waveform

This waveform suggests a system experiencing transient behavior at the start, potentially due to startup or load changes, followed by a relatively stable operation with minor voltage variations, possibly reflecting ripple or control adjustments. The overall voltage trend indicates a DC signal with some superimposed AC components or control-induced fluctuations.

The Figure 7 presents two sets of three-phase waveforms. The **upper plot** of figure 6 shows three sinusoidal voltage waveforms, each with a peak amplitude of approximately 10V (positive and negative). These waveforms are phase-shifted by 120 degrees, characteristic of a balanced three-phase system, and exhibit a consistent frequency. The **lower plot** displays three sinusoidal current waveforms. These currents are also phase-shifted by 120 degrees, indicating a balanced load, and have a peak amplitude of roughly 0.2A (positive and negative). Both sets of waveforms demonstrate the expected behavior of a three-phase system, with synchronized and phase-displaced sinusoidal patterns. The consistent amplitudes and phase relationships suggest a stable and balanced three-phase operation.

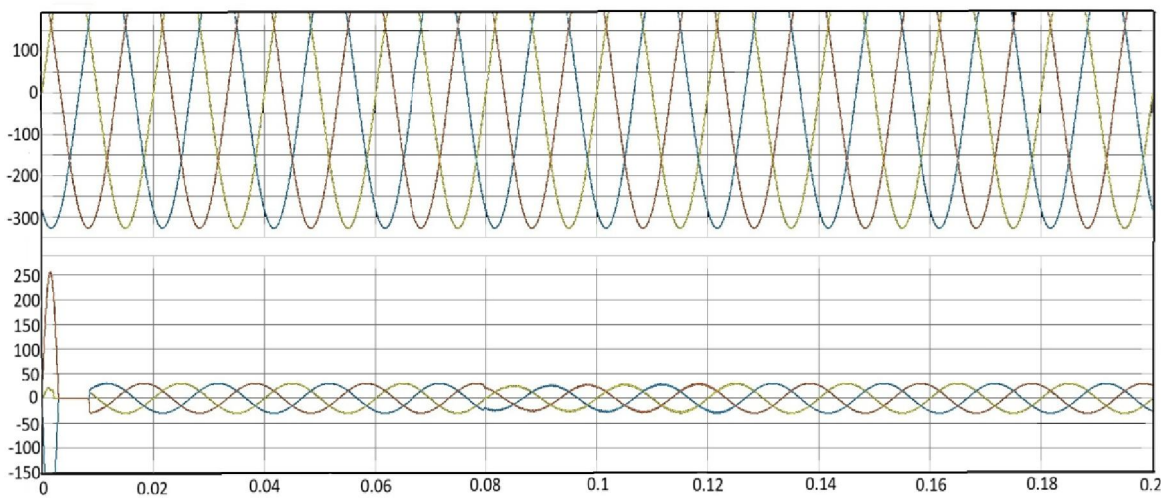


Fig.7. 3-phase AC Voltage and Current wave forms

**Table I: Parameters description**

Parameter	Value (Approximate)	Units	Description
Peak Voltage	10	V	Maximum amplitude of each phase voltage
Phase Shift	120	Degrees	Angular displacement between phase voltages
Peak Current	0.2	A	Maximum amplitude of each phase current
Phase Shift	120	Degrees	Angular displacement between phase currents
Initial Peak Voltage	480	V	Maximum voltage at startup
Average Voltage	420	V	Approximate mean voltage after stabilization
Voltage Fluctuation Range	410 - 430	V	Range of voltage variation during operation
Initial SOC	1	%	State of charge at the beginning
Final SOC	27	%	State of charge at the end
SOC Increase	26	%	Total increase in state of charge

## V. CONCLUSION AND FUTURE SCOPE

The feasibility of a dynamic wireless power transfer (WPT) system for electric vehicles (EVs) utilizing a VEENA Rectifier and a single-phase AC-DC converter subsystem. The battery state-of-charge (SOC) graph shows a consistent linear increase, indicating effective charging. The DC voltage waveform, while exhibiting initial transients and slight fluctuations, stabilizes around an average value, suggesting successful DC voltage regulation. The three-phase



waveforms confirm a balanced and stable three-phase system operation. The results support the abstract's claim of achieving stable and efficient power transfer, particularly with the observed linear increase in SOC. The VEENA Rectifier and AC-DC converter subsystem appear to function as intended, contributing to the overall system performance. However, the initial transients in the DC voltage waveform suggest a need for further optimization of the control algorithms and component selection.

Future work can focus on implementing and simulating the system with two receiver coils, as initially proposed. This would involve modeling the coupling and interactions between the two coils and evaluating the system's performance under various misalignment scenarios

#### REFERENCES

- [1]. Gandoman FH, Van Mierlo J, Ahmadi A, Abdel Aleem SHE, Chauhan K. Safety and Reliability Evaluation for Electric Vehicles in Modern Power System Networks. *Distrib. Energy Resour. Microgrids*, Elsevier 2019:389–404. doi: 10.1016/B978-0-12-817774-7.00015-6.
- [2]. Sharaf AM, Omar N, Gandoman FH, Zobaa AF, Abdel Aleem SHE. Electric and Hybrid Vehicle Drives and Smart Grid Interfacing. *Adv. Renew. Energies Power Technol.*, vol. 2, Elsevier; 2018, p. 413–39. doi: 10.1016/B978-0-12-813185-5.00008-5.
- [3]. Naoui M, Aymen F, Ben Hamed M, Lassaad S. Analysis of Battery-EV State of Charge for a Dynamic Wireless Charging System. *Energy Storage* 2019; 2:1–10. doi: 10.1002/est.2.117.
- [4]. Triviño-Cabrera A, Ochoa M, Fernández D, Aguado JA. Independent Primary Side Controller Applied to Wireless Chargers for Electric Vehicles. *IEEE Int Electr Veh Conf IEVC*. doi: 10.1109/IEVC.2014.7056193.
- [5]. Mohamed N, Aymen F, Issam Z, Bajaj M, Ghoneim SSM. The Impact of Coil Position and Number on Wireless System Performance for Electric Vehicle Recharging. *Sensors* 2021; 21:1–19. doi: 10.3390/s21134343.
- [6]. Castilla M, Miret J, Matas J, de Vicuña LG, Guerrero JM. Control Design Guidelines for Single-Phase Grid-Connected Photovoltaic Inverters with Damped Resonant Harmonic Compensators. *IEEE Trans Ind Electron* 2009; 56:4492–501. doi: 10.1109/TIE.2009.2017820.
- [7]. Mousa AGE, Abdel Aleem SHE, Ibrahim AM. Mathematical Analysis of Maximum Power Points and Currents Based Maximum Power Point Tracking in Solar Photovoltaic System: a Solar Powered Water Pump Application. *Int Rev Electr Eng* 2016; 11(97). doi: 10.15866/iree.v11i1.8137.
- [8]. Sudimac B, Ugrinović A, Jurčević M. The Application of Photovoltaic Systems in Sacred Buildings for the Purpose of Electric Power Production: The Case Study of the Cathedral of St. Michael the Archangel in Belgrade. *Sustain* 2020; 12. doi: 10.3390/su12041408.
- [9]. Asna M, Shareef H, Achikkulath P, Mokhlis H, Errouissi R, Wahyudie A. Analysis of an Optimal Planning Model for Electric Vehicle Fast-Charging Stations in Al Ain City, United Arab Emirates. *IEEE Access* 2021; 9:73678–94. doi: 10.1109/access.2021.3081020.
- [10]. Savari GF, Krishnasamy V, Sathik J, Ali ZM, Abdel Aleem SHE. Internet of Things-Based Real-Time Electric Vehicle Load Forecasting and Charging Station Recommendation. *ISA Trans* 2020; 97:431–47. doi: 10.1016/j.isatra.2019.08.011.
- [11]. Jahangir H, Tayarani H, Ahmadian A, Golkar MA, Miret J, Tayarani M, et al. Charging Demand of Plug-in Electric Vehicles: Forecasting Travel Behavior Based on a Novel Rough Artificial Neural Network Approach. *J Clean Prod* 2019; 229:1029–44. doi: 10.1016/j.jclepro.2019.04.345.
- [12]. Younes Z, Alhamrouni I, Mekhilef S, Reyasudin M. A Memory-Based Gravitational Search Algorithm for Solving Economic Dispatch Problem in Micro-grid. *Ain Shams Eng J* 2021; 12:1985–94. doi: 10.1016/j.asej.2020.10.021.
- [13]. Hussien AM, Hasanien HM, Mekhamer SF. Sunflower Optimization Algorithm-Based Optimal PI Control for Enhancing the Performance of an Autonomous Operation of a Microgrid. *Ain Shams Eng J* 2021; 12:1883–93. doi: 10.1016/j.asej.2020.10.020.

- [14]. Sobhy MA, Abdelaziz AY, Hasanien HM, Ezzat M. Marine Predators Algorithm for Load Frequency Control of Modern Interconnected Power Systems Including Renewable Energy Sources and Energy Storage Units. *Ain Shams Eng J* 2021. doi: 10.1016/j.asej.2021.04.031.
- [15]. Mostafa MH, Aleem SHEA, Ali SG, Abdelaziz AY, Ribeiro PF, Ali ZM. Robust Energy Management and Economic Analysis of Microgrids Considering Different Battery Characteristics. *IEEE Access* 2020; 8:54751–75. doi: 10.1109/ACCESS.2020.2981697.
- [16]. Rawa M, Abusorrah A, Bassi H, Mekhilef S, Ali ZM, Abdel Aleem SHE, et al. Economical-Technical-Environmental Operation of Power Networks with Wind-Solar-Hydropower Generation Using Analytic Hierarchy Process and Improved Grey Wolf Algorithm. *Ain Shams Eng J* 2021. doi: 10.1016/j.asej.2021.02.004.
- [17]. Cálasan M, Zobaa AF, Hasanien HM, Aleem SHEA, Ali ZM. Towards Accurate Calculation of Supercapacitor Electrical Variables in Constant Power Applications Using New Analytical Closed-Form Expressions. *J Energy Storage* 2021; 42:102998.
- [18]. Ji B, Song X, Cao W, Pickert V, Hu Y, Mackersie JW, et al. In-situ Diagnostics and Prognostics of Solder Fatigue in IGBT Modules for Electric Vehicle Drives. *IEEE Trans Power Electron* 2015; 30:1535–43. doi: 10.1109/TPEL.2014.2318991.
- [19]. Ma G, Kamaruddin MH, Kang HS, Goh PS, Kim MH, Lee KQ, et al. Watertight Integrity of Underwater Robotic Vehicles by Self-Healing Mechanism. *Ain Shams Eng J* 2021; 12:1995–2007. doi: 10.1016/j.asej.2020.09.019.
- [20]. Erdogan A, Kizilkan O, Colpan CO. Thermodynamic Performance Assessment of Solar-Based Closed Brayton Cycle for Different Supercritical Fluids. *Int Conf Smart Sustain Technol Split* 2019; 2019, p. 0–4. doi: 10.23919/SpliTech.2019.8783142.